Molecular Mechanism of Sequence-Specific Termination of Lentiviral Replication†

Anthony J. Berdis,*,⊥ Scott R. Stetor,‡,§ Stuart F. J. LeGrice,‡,|| and Mary D. Barkley#

USA Division of Infectious Diseases, Department of Medicine, and Departments of Pharmacology and Chemistry, Case Western Reserve University, Cleveland, Ohio 44106

Received February 20, 2001; Revised Manuscript Received May 30, 2001

ABSTRACT: The central termination sequence (CTS) terminates (+) strand DNA synthesis in certain lentiviruses. The molecular mechanism underlying this event, catalyzed by equine infectious anemia virus reverse transcriptase (EIAV RT), was evaluated by pre-steady-state kinetic techniques. Time courses in nucleotide incorporation using several DNA substrates were biphasic, consistent with release of enzyme from extended DNA being the rate-limiting step for turnover. While the burst amplitude reflecting the amount of functional RT−DNA complex was sequence-dependent, rate constants for initial product formation were not. Filter binding assays indicate the K_d for CTS-containing substrate is only 2-fold higher than a random DNA and cannot account entirely for the large diminution in burst amplitudes. Measurements of processive DNA replication on a millisecond time scale indicate that the rate of polymerization is unaffected by the T_6-tract within the CTS. However, termination products accumulate due to a substantial increase in the rate of nonproductive enzyme−nucleic acid complex formation after incorporation of four to five adenosines of a T_6-tract within the CTS. During strand displacement synthesis through the CTS, products accumulate after incorporation of three to four adenosines. The rate of polymerization during strand displacement synthesis decreases 2-fold while the rate of nonproductive enzyme−nucleic acid complex formation is identical in the absence or presence of the displacement strand. These results have allowed us to develop a model for CTS-induced termination of (+) strand synthesis.

All retroviruses must convert their plus (+) strand RNA genomes into double-stranded DNA through the activity of a virally encoded reverse transcriptase. RT[1] is a unique polymerase since it must efficiently perform replication on a variety of nucleic acid substrates and conformations. For example, RT initiates (−) strand DNA synthesis on an RNA/RNA duplex, the primer of which is a host-derived tRNA. Once initiated, (−) strand DNA synthesis generates a DNA/RNA hybrid, the RNA component of which is concomitantly degraded through the hydrolytic activity of the RT-associated RNase H component. (+) strand DNA synthesis is initiated from the RNase H-resistant RNA/DNA segment designated the PPT. This sequence is almost exclusively composed of purine residues immediately upstream of U_3 (*1*−*3*). Similar to the situation in HIV, the EIAV genome was shown to contain two PPT sequences, namely, the 3′-PPT analogous to that found in all retroviruses and a second designated the central PPT (cPPT) (*4*). Thus, certain lentiviruses appear to support (+) strand DNA synthesis in two discrete steps at the center and 3′-end of their genomes. According to the model proposed by Charneau et al. (*4*) for HIV-1 replication, elongation from the 3′-PPT provides (+) strong stop DNA, while cPPT-primed synthesis continues to the end of the template. Following second strand transfer, 3′-PPT-primed synthesis is renewed and continues to the center of the genome at which stage RT displaces a short segment (∼90 bases) of duplex DNA. The consequence of this is a discontinuous (+) strand DNA with an overlapping, single-stranded DNA flap of 90 bases (*5*). Although RT lacks a DNA cleavage activity to alleviate this structure (reviewed in ref *6*), it could be rapidly removed in vitro by a host endonuclease, Flap endonuclease-1 (*7*). The remaining gap in the DNA would then be repaired by host DNA polymerase and DNA ligase (*7*).

This mode of discontinuous synthesis of the viral (+) strand requires an additional mechanism for terminating the polymerizing complex as synthesis of proviral DNA nears completion. The *cis*-acting element that performs this function in HIV-1 was originally identified and designated the central termination sequence (CTS). This region lies 90 base pairs downstream from the cPPT (*5*, *8*) and is defined by phased A-tracts which induce global curvature of the DNA helix (*9*, *10*). We have previously examined, through steady-state kinetic analyses, the consequences of EIAV DNA synthesis upon encountering its counterpart of the HIV CTS

† This work was supported through NIH Grant GM52263.

* Corresponding author. Telephone: (216) 368-6255. Fax: (216) 368-3395. E-mail: ajb15@po.cwru.edu.

⊥ Department of Pharmacology, Case Western Reserve University.

‡ Department of Medicine, Case Western Reserve University.

§ Present address: Bio-Rad Laboratories, 2000 Alfred Nobel Drive, Hercules, CA 94547.

|| Present address: Resistance Mechanisms Laboratory, HIV Drug Resistance Program, National Cancer Institute—Frederick, Frederick, MD.

Department of Chemistry, Case Western Reserve University.

[1] Abbreviations: cPPT, central polypurine tract; CTS, central termination sequence; dNTP, deoxynucleotide triphosphate; EDTA, ethylenediaminetetraacetic acid; EIAV, equine infectious anemia virus; HIV-1, human immunodeficiency virus type 1; k_{int}, rate constant for intermediate product formation; k_{ext}, rate constant for primer extension; k_{cat}, turnover number; K_d, equilibrium binding constant; k_{obs}, rate constant for initial product formation; k_{pol}, maximal rate of DNA polymerization; KF, Klenow fragment of *Escherichia coli* DNA polymerase I; PPT, polypurine tract; RT, reverse transcriptase; 3′-PPT, 3′-polypurine tract; TBE, Tris−borate−EDTA.

10.1021/bi010354i CCC: $20.00
Published on Web 09/15/2001

Scheme 1: Simplified Reaction Mechanism Representing the Sequential Conversion of Potential Substrates into Products during Processive DNA Replication Catalyzed by EIAV RT[a]

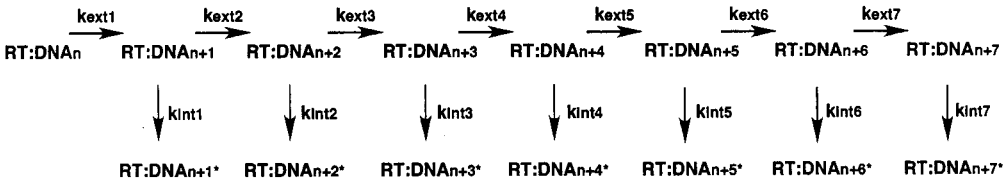

[a] This mechanism allows for the analysis of the rate at which potential substrate is converted into product (k_{ext1}) that can then be subsequently utilized (k_{ext2}) as well as the rate at which potential substrate is converted into an intermediate product from which extension does not occur (k_{int1}) and so forth. The kinetic steps for dNTP binding, the conformational change before and after chemistry, and phosphoryl transfer are combined and are denoted as k_{ext}.

(*11*). These studies demonstrated that the A-tract DNA of the EIAV CTS, although not in phase, possessed a unique structural conformation which efficiently terminated DNA synthesis. In support of this notion, incorporation of the nucleoside analogue 2,6-diaminopurine alleviated termination at this sequence, presumably by abolishing minor groove compression within A-tracts.

While these data indicate that minor groove compression plays a role in termination of lentiviral DNA synthesis, the molecular mechanism by which the activity of RT is perturbed remains elusive. An attractive model to account for sequence-specific termination is that minor groove compression disrupts the intimate contacts between the enzyme and nucleic acid to induce its dissociation at the CTS. Alternatively, steric constraints imposed by minor groove compression may not promote dissociation but facilitate formation of a nonproductive enzyme complex remaining bound to the substrate but unable to perform DNA synthesis. To differentiate between these mechanisms, pre-steady-state analysis of nucleotide incorporation catalyzed by EIAV RT was employed using DNA substrates of random sequence as well as DNA containing the CTS region of the EIAV genome. By determining the individual rate constants for DNA replication through the CTS, we were able to pinpoint which steps were affected as a function of nucleic acid substrate. DNA synthesis by EIAV RT during strand displacement was also evaluated on the millisecond time scale using a forked DNA substrate composed of the CTS sequence. On the basis of quantitative analysis of the pre-steady-state data, a model is provided to explain the molecular mechanism of sequence-dependent termination of lentiviral DNA replication.

MATERIALS AND METHODS

Materials. All general reagents and buffers were purchased from Sigma. dNTPs (>98% purity) were from Pharmacia. Nitrocellulose filters were from Bio-Rad and DEAE filters from Whatman. The Minifold I Dot-Blot system used in filter binding assays was from Schleicher and Schuell. Oligonucleotides were obtained from IDT (Iowa) and Operon Technologies (Almeda, CA). [γ-^{32}P]ATP and [α-^{32}P]dCTP were purchased from Dupont/NEN (Boston, MA) and ICN Biomedicals (Irvine, CA). EAIV and HIV-1 RT were purified and quantified as previously described (*12*, *13*). The Klenow fragment of DNA polymerase I of *Escherichia coli* was purified and quantified as previously described (*14*). Single-stranded and duplex DNA were purified and quantified as described (*15*, *16*). Concentrations of all duplex DNA substrates were determined by measuring the enzymatic incorporation of [α-^{32}P]dNTP as previously described (*15*).

Kinetic Analyses. Rapid-quench experiments were carried out in a rapid-quench apparatus (KinTek Corp., State College, PA) as described by Johnson (*17*). Pre-steady-state reactions were conducted under pseudo-first-order reaction conditions in which ^{32}P-labeled DNA was in excess relative to the enzyme.

(A) Single Nucleotide Incorporation Analysis. A typical experiment was performed in which 200 nM EIAV RT p66/p51 heterodimer was preincubated with 500 nM DNA substrate in a solution of 50 mM Tris-HCl, 10 mM $MgCl_2$, 80 mM KCl, and 5 mM DTT (RT reaction buffer). The preformed RT−DNA complex was mixed with a solution containing the appropriate dNTP (100 μM final concentration) and quenched with a 500 mM EDTA solution at times varying from 0.005 to 5 s. The final volumes of the reactions were normalized by adding appropriate volumes of 500 mM EDTA to the collection tubes. Aliquots from the reactions were added to an equal volume of formamide loading buffer (90% formamide, 10% 10× TBE, 0.025% bromophenol blue, 0.025% xylene cyanol). Products were separated using denaturing gel electrophoresis, imaged using a PhosphorImager (Molecular Dynamics), and quantified using ImageQuant software supplied by the manufacturer. Product formation was quantified by measuring the ratio of ^{32}P-labeled extended and nonextended primers. The ratios of product formation are corrected for substrate in the absence of polymerase. Corrected ratios are then multiplied by the concentration of primer/template used in each assay to yield total product and are listed as final solution concentrations. Data obtained for pre-steady-state DNA polymerization measurements were fit to the equation:

$$y = Ae^{-kt} + Bt + C \quad (1)$$

where A is the burst amplitude, k is the first-order rate constant for initial product formation (k_{obs}), B is the steady-state rate, t is time, and C is a defined constant.

(B) Processive DNA Replication Assay. Processive dNTP incorporation was performed using the rapid quench instrument as described above. In these experiments, dCTP and dATP (100 μM each) were used with 30/60-mer and 30/60/44-mer substrates while dCTP, dGTP, and dATP (100 μM each) were used with the 25/36-mer substrate. Simulations modeling the observed kinetic time courses for nucleotide incorporation were performed by mathematical analyses to the simplified mechanism depicted in Scheme 1 using KINSIM (*18*). Both the starting reactant concentrations and rate constants were supplied for each step of the mechanism. Rate constants were either determined experimentally or based upon published values. Using this information, the

unknown rate constants were defined through computer fits of the time courses in product formation. Simulated curves were then compared to the experimental curves to judge how accurately the set of rate constants simulate the experimental data. Adjustments to the rate constants were made until the simulated time courses were nearly identical to the experimental time courses. The iterative nonlinear regression analysis program FITSIM was then used to predict how well the mechanism and the set of rate constants describe the experimental data.

(C) Trap Extension Assays. The preformed RT−DNA complex (300 nM RT and 300 nM 30/60-mer or 30/60/44-mer) was rapidly mixed with 3 μM DNA trap and dCTP and dATP (100 μM final concentration) for times ranging from 0.01 to 5 s. Trap was 25/36-mer whose 25-mer primer was 5′-labeled. Products were analyzed for the extension of the 30/60-mer or 30/60/44-mer as well as extension of the 25/36-mer DNA trap. Data were analyzed as described above.

Determination of the Equilibrium Dissociation Constant, K_d, for DNA Substrates. Filter binding assays were performed as previously described (*19*, *20*) to measure the equilibrium dissociation constant, K_d, for various DNA substrates. Nitrocellulose and DEAE filters were placed on a Minifold I Dot-Blot system, allowing samples to sequentially pass through the nitrocellulose and then the DEAE filter. Assays were performed in a final volume of 50 μL using a fixed RT concentration (20 nM) while varying the concentration of DNA from 0 to 200 nM. Reactions were incubated for 5 min at 37 °C to allow equilibration of enzyme with DNA. Immediately before the samples were filtered, the wells were flushed with 100 μL of RT buffer. A vacuum was applied to draw the flush solution through the membrane. Samples were then loaded and the vacuum was reapplied. The wells were subsequently washed with another 100 μL of RT buffer, after which membranes were imaged using a PhosphorImager (Molecular Dynamics) and quantified using ImageQuant software supplied by the manufacturer.

The concentration of DNA−RT complex thus obtained was calculated using the equation:

$$[\mathrm{DNA}]_{\mathrm{bound}} = [[\mathrm{DNA}]_{\mathrm{total}}(\mathrm{cpm}_{\mathrm{NC}} - \mathrm{bkg}_{\mathrm{NC}})]/(\mathrm{cpm}_{\mathrm{NC}} + \mathrm{cpm}_{\mathrm{DEAE}}) \quad (2)$$

where $[\mathrm{DNA}]_{\mathrm{bound}}$ represents the concentration of the DNA−RT complex, $[\mathrm{DNA}]_{\mathrm{total}}$ represents total DNA concentration for each binding reaction, $\mathrm{bkg}_{\mathrm{NC}}$ represents the amount of nonspecific DNA binding, and $\mathrm{cpm}_{\mathrm{NC}}$ and $\mathrm{cpm}_{\mathrm{DEAE}}$ represent binding on nitrocellulose and DEAE filters, respectively. The K_d for DNA substrate was obtained using the quadratic equation:

$$[\mathrm{E{-}DNA}] = 0.5(K_d + [\mathrm{E}] + [\mathrm{DNA}] - [0.25(K_d + [\mathrm{E}] + [\mathrm{DNA}])^2 - \mathrm{E{-}DNA}]^{1/2} \quad (3)$$

where [E] is the concentration of RT, [DNA] the concentration of DNA, [E−DNA] the amount of DNA bound by enzyme, and K_d the equilibrium binding constant for DNA.

RESULTS

Defined DNA Substrates. Figure 1 displays the duplex DNA substrates utilized in this study to characterize replication catalyzed by EIAV RT. The 30/60-mer duplex substrate

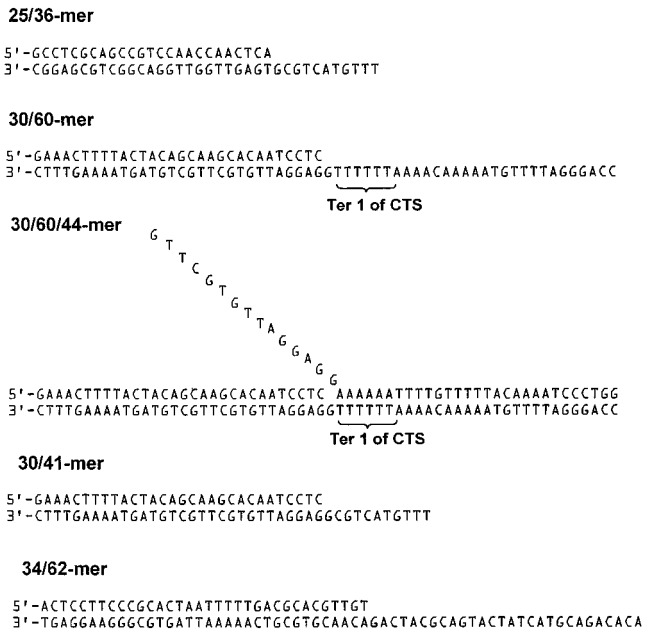

FIGURE 1: Sequences of DNA substrates utilized for kinetic analysis of DNA polymerization activity.

contains the primary pause site of the CTS immediately downstream of the 3′ terminus of the primer and mimics DNA encountered during in vivo synthesis in the context of early (+) strand DNA synthesis. A forked DNA substrate containing a 44-mer oligonucleotide annealed to the 30/60-mer substrate downstream was designed to mimic forked DNA encountered in vivo in the context of late plus (+) strand DNA synthesis. The 44-mer oligonucleotide is composed of two regions: a 3′ region (29 nucleotides) complementary to the 60-mer template and a noncomplementary 5′ region (15 nucleotides). A 25/36-mer duplex oligodeoxynucleotide substrate not containing the EIAV CTS is similar to that used to characterize HIV-1 RT (*21*) and was employed as a control. Likewise, a 34/62-mer substrate not containing the EIAV CTS was employed to evaluate the effects of duplex length as well as single-stranded length. An additional control substrate is the 30/41-mer in which the template contains the first 30 nucleotides of the 60-mer template (CTS-containing) with the final 11 nucleotides of the non-CTS-containing template.

Evaluation of the EIAV RT Kinetic Mechanism. Pre-steady-state kinetics monitoring elongation of the 25/36-mer substrate to a 26/36-mer product were performed under pseudo-first-order conditions to examine the kinetic mechanism of DNA-dependent DNA polymerase activity of EIAV RT. The time course in product formation is biphasic with a rapid burst in product accumulation followed by a slower, linear steady-state phase (Figure 2).[2] The pattern is consistent with a two-step kinetic mechanism in which binding of dNTP and phosphoryl transfer occur rapidly followed by regeneration

[2] It was previously reported (*12*) that the burst amplitude of EIAV RT consists of a fast and a slower phase followed by a steady-state phase. Under pseudo-first-order conditions, we observe only one burst phase followed by a steady-state phase. Likewise, one burst phase is observed when the reaction is performed using single turnover conditions, i.e., RT in molar excess versus DNA substrate (data not shown). The reason for this difference is presently unclear but may reflect the utilization of different DNA sequences and/or higher DNA concentrations for each active site titration.

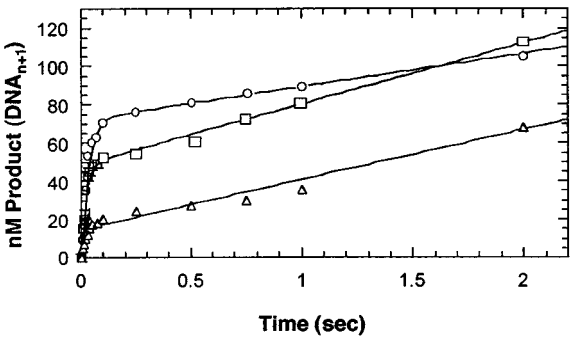

FIGURE 2: Time courses for single nucleotide incorporation into 25/36-mer (○), 30/60-mer (□), and 30/60/44-mer (△) DNA substrates by EIAV RT. Time courses in dCTP incorporation were performed in a rapid quench instrument by mixing the preformed RT−DNA complex with 100 μM dCTP. A final concentration of 500 nM DNA substrate was used in all cases. The final concentration of EIAV RT was 150 nM using the 25/36-mer and 200 nM using the 30/60-mer and 30/60/44-mer DNA substrates. The reaction was then terminated at the times designated by the addition of 500 mM EDTA.

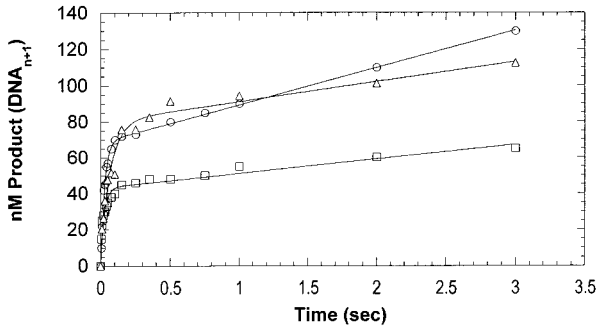

FIGURE 3: Pre-steady-state kinetics for incorporation of dCTP by EIAV RT using 25/36-mer (○), 30/41-mer (□), and 34/62-mer (△). Time courses in dCTP incorporation were performed in a rapid quench instrument by mixing the preformed RT−DNA complex with 100 μM dCTP. A final concentration of 500 nM DNA substrate was used in all cases. The final concentration of EIAV RT was 150 nM using the 25/36-mer and 34/62-mer DNA substrates while 200 nM was employed using the 30/41-mer DNA substrate. The reaction was then terminated at the times designated by the addition of 500 mM EDTA.

of free enzyme in a second rate-limiting step. The burst amplitude is 70 ± 2 nM, approximately 50% of the final enzyme concentration. Similar results have been reported with HIV-1 RT (*21*−*23*), suggesting that 50% of the enzyme is either inactive or binds nonproductively to the DNA substrate. The rate of initial product formation (k_{obs}) is 33 ± 5 s^{-1}. The linear steady-state phase is presumed to reflect the rate-limiting step of RT dissociation from the extended primer from which a turnover rate, k_{cat}, of 0.24 ± 0.02 s^{-1} was measured.

Kinetics of Single Nucleotide Incorporation Using CTS-Containing Substrates. A series of single dNTP incorporation experiments were performed using the 30/60-mer and 30/60/44-mer substrates to investigate the kinetics of polymerization on substrates mimicking the CTS. Using either substrate, a rapid burst in product formation is followed by a linear steady-state rate (Figure 2) as was observed using the 25/36-mer control substrate. The burst amplitudes were 45 ± 1 and 23 ± 3 nM for 30/60-mer and 30/60/44-mer, respectively, and represent 23% and 12%, respectively, of the expected values based on protein concentration. The decrease in burst amplitudes suggests that the enzyme is unable to bind to the 30/60-mer and 30/60/44-mer as efficiently as the 25/36-mer. Values for k_{obs} were determined to be 37 ± 6 and 26 ± 12 s^{-1} for 30/60-mer and 30/60/44-mer substrates, respectively, and are in good agreement with the k_{obs} value of 33 ± 5 s^{-1} measured using the 25/36-mer as the substrate. Turnover rates (k_{cat}) were 0.67 ± 0.03 and 1.5 ± 0.1 s^{-1} for 30/60-mer and 30/60/44-mer substrates, respectively.

The time course in dCTP incorporation was performed using the "hybrid" 30/41-mer substrate in which the CTS region is replaced with a random sequence. The burst amplitude value of 43 ± 7 nM represents 22% of the expected value based on protein concentration (Figure 3). The burst rate of 33 ± 3 s^{-1} and k_{cat} of 0.33 ± 0.05 s^{-1} also agree well with those measured for the 30/60-mer substrate. By contrast, the time course in dCTP incorporation using the 34/62-mer substrate yields a burst amplitude of 72 ± 6 nM representing 48% of the expected value based on protein concentration (Figure 3). The burst rate of 22 ± 5 s^{-1} and k_{cat} of 0.15 ± 0.02 s^{-1} also agree well with those measured for the 25/36-mer substrate. A summary of kinetic constants for EIAV RT using the various DNA substrates is provided in Table 1.

Time courses in dCTP incorporation were likewise performed using HIV-1 RT and Klenow fragment to evaluate if the CTS sequences affect other DNA polymerases. Values for burst amplitudes, k_{obs}, and k_{cat} for both enzymes are presented in Table 2. Surprisingly, we found that both enzymes display a 2-fold reduction in burst amplitude using the 30/60-mer compared to the 25/36-mer. Although k_{obs} values are essentially independent of substrate, the k_{cat} of both enzymes is 2-fold higher using the 30/60-mer compared to the 25/36-mer.

Processive DNA Synthesis Catalyzed by EIAV RT. (A) 25/36-mer. Processive polymerization by EIAV RT was investigated by including three dNTPs in the reaction mixture, allowing elongation of the 25/36-mer substrate to a +5 product. An excess of 5′-labeled 25/36-mer over enzyme assured that the kinetics of sequential elongation events resulted from a single enzyme-binding event. The reaction products are presented in Figure 4A, and the quantified time courses are presented in Figure 4B. Polymerization occurs in a sequential, time-dependent manner as initial substrate (25-mer) is converted to full-length product (30-mer). Similar to HIV-1 RT (21), EIAV RT appears to be dissociative in nature since intermediate products (26- through 29-mers) are not completely converted to full-length 30-mer product. However, the major product that accumulates over time is the full-length +5 product as is expected since only three dNTPs are provided in the reaction.

Computer simulation of the time course to the reaction mechanism depicted in Scheme 1 yielded rate constants for primer elongation as well as for accumulation of intermediate products. These data, summarized in Table 3, reveal that the rate constants for primer elongation remain fairly constant at ∼25 s^{-1}. In contrast, rate constants reflecting intermediate product formation tend to increase as primer elongation increases. These rate constants may reflect enzyme dissociation or the formation of RT−DNA complexes that are nonproductive. Since this issue cannot be resolved on the

Table 1: Comparison of Kinetic Constants for DNA Polymerization of EIAV RT Using 25/36-mer, 30/60-mer, 30/60/44-mer, 30/41-mer, or 34/62-mer DNA Substrates[a]

	25/36-mer	30/60-mer	30/60/44-mer	30/41-mer	34/62-mer
burst amplitude (nM)	70 ± 2	45 ± 1	23 ± 3	43 ± 7	72 ± 6
% enzyme[b]	47	23	12	22	48
k_{obs} (s^{-1})	33 ± 5	37 ± 6	26 ± 12	33 ± 3	22 ± 5
k_{cat}[c] (s^{-1})	0.24 ± 0.02	0.67 ± 0.03	1.5 ± 0.1	0.33 ± 0.05	

[a] Time courses in dCTP incorporation were performed in a rapid quench instrument by mixing the preformed RT−DNA complex with 100 μM dCTP. 500 nM DNA substrate was used in all cases. The concentration of EIAV RT was 150 nM using the 25/36-mer and 34/62-mer DNA substrates or 200 nM using the 30/60-mer, 30/60/44-mer, and 30/41-mer DNA substrates. [b] Percent enzyme reflects the burst amplitude (functional enzyme) divided by the total molar concentration of enzyme present in the reaction. [c] k_{cat} values were obtained by dividing the steady-state rate of nucleotide incorporation by the obtained burst amplitude.

Table 2: Kinetic Constants for DNA Polymerization of HIV-1 RT and Klenow Fragment Using the 25/36-mer or 30/60-mer DNA Substrate[a]

	HIV-1 RT		Klenow fragment	
	25/36-mer	30/60-mer	25/36-mer	30/60-mer
burst (nM)	87 ± 7	42 ± 2	110 ± 6	48 ± 1
% enzyme[b]	58	28	110	48
k_{obs} (s^{-1})	56 ± 11	41 ± 4	16 ± 1	25 ± 2
k_{cat}[c] (s^{-1})	0.28 ± 0.03	0.52 ± 0.02	0.46 ± 0.04	0.25 ± 0.02

[a] Time courses in dCTP incorporation were performed as described in Materials and Methods. The concentration of HIV-1 RT was 150 nM using the 25/36-mer DNA substrate and 200 nM using the 30/60-mer DNA substrate. The concentration of Klenow fragment was 100 nM using either the 25/36-mer or 30/60-mer DNA substrate. [b] Percent enzyme reflects the burst amplitude (functional enzyme) divided by the total molar concentration of enzyme present in the reaction. [c] k_{cat} values were obtained by dividing the steady-state rate of nucleotide incorporation by the obtained burst amplitude.

basis of the current data, these rate constants are temporarily assigned as k_{int}.

(B) 30/60-mer. Processive DNA synthesis through the CTS (Figure 5) is similar in nature to that using 25/36-mer, i.e., sequential and time-dependent conversion of initial substrate into longer products. A notable difference, however, is that +5 and +6 products accumulate while the full-length product (+7) severely lags in formation throughout the time course. These data provide the first definitive demonstration that significant pausing occurs prior to completion of replication of the A-tract in the CTS.

A surprising feature is that the rate constants reflecting primer elongation remain essentially constant (~20−30 s^{-1}) and very similar to those obtained using the 25/36-mer substrate (Table 2). More important is the marked increase in k_{int} relative to k_{ext}, especially when compared to those obtained using the 25/36-mer. A pronounced increase in k_{int} relative to k_{ext} occurs at the +5 product (35/60-mer) and +6 product (36/60-mer) and likely reflects the drastic accumulation of these intermediate products. Identical results were obtained when RT was provided with all dNTPs required for complete elongation of the primer, confirming that pausing at Ter 1 is sequence specific and independent of artificially stalling RT at the CTS through nucleotide omission.

(C) 30/60/44-mer. Strand displacement synthesis through the CTS was next measured to evaluate the role of the displacement strand in termination of DNA synthesis. The time course (data not shown) revealed accumulation of +4 and +5 products as opposed to the accumulation of +5 and +6 products observed in the absence of strand displacement.

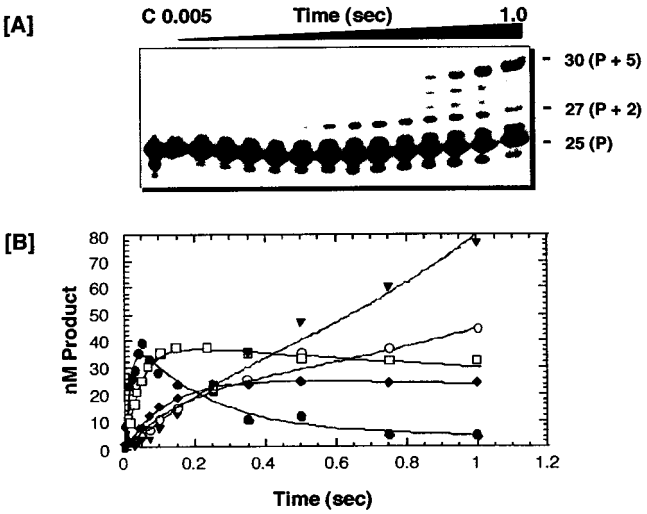

FIGURE 4: Processive DNA synthesis by EIAV RT using the 25/36-mer DNA substrate. (A) Reaction products separated on a 16% denaturing polyacrylamide gel. Assays were performed in which a preincubated solution of 100 nM EIAV RT p66/p51 heterodimer was preincubated with 500 nM DNA substrate and was mixed with dCTP and dATP (100 μM each). The reaction was then terminated by the addition of 500 mM EDTA at times encompassing 0.005 to 1 s. For convenience, only the initial substrate (P) and extended product (P + 2 and P + 5, respectively) are denoted. (B) Data obtained from PhosphorImager analysis of gel electrophoresis displaying the sequential accumulation of intermediate products followed by the accumulation of the terminal +5 product. Product formation is denoted as follows: ● = +1 product, □ = +2 product, ◆ = +3 product, ○ = +4 product, and ▼ = +5 product. The curves for product formation were generated using the rate constants denoted in Table 3, which were obtained through computer simulation of the experimental data to Scheme 1.

Furthermore, although the primer should be extended to a full-length +7 product, products longer than +5 are not observed. Values for k_{ext}, summarized in Table 3, vary from 5 to 20 s^{-1}. These values are approximately 2-fold lower than those obtained in the absence of the displacement strand. Although k_{int} increases relative to the incorporation rate constants, the values are essentially identical to those obtained in the absence of strand displacement. During strand displacement, k_{int} eclipses k_{ext} at the +4 and +5 products to cause the accumulation of these intermediate products.

Kinetics of Enzyme Dissociation. The formation of intermediate products has to this point been simply defined as an ambiguous rate constant denoted as k_{int}. As previously discussed, this may reflect enzyme dissociation or the formation of nonproductive RT−DNA complexes. Distinction between these two possibilities is important for accurately defining the kinetic consequence of RT encountering the unique structure of the CTS. We therefore monitored

Table 3: Summary of Kinetic Rate Constants for DNA Polymerization and Nonproductive Complex Formation during Processive DNA Replication[a]

position	25/36-mer		30/60-mer		30/60/44-mer	
	k_{ext} (s^{-1})[b]	k_{int} (s^{-1})[c]	k_{ext} (s^{-1})	k_{int} (s^{-1})	k_{ext} (s^{-1})	k_{int} (s^{-1})
+1	35 ± 5	0.7 ± 0.1	35 ± 8	0.5 ± 0.1	15 ± 2	0
+2	25 ± 3	3.7 ± 0.4	18 ± 4	0.3 ± 0.1	7 ± 1	0
+3	18 ± 4	4.5 ± 1.0	15 ± 3	1.5 ± 0.3	5 ± 1	1.5 ± 0.3
+4	25 ± 8	9.1 ± 3.2	25 ± 5	5 ± 1	14 ± 3	7 ± 1
+5	25 ± 8	ND[d]	30 ± 7	17 ± 4	15 ± 1	20 ± 1
+6	ND	ND	30 ± 2	45 ± 3	20 ± 2	5.0 ± 1.5
+7	ND	ND	30 ± 7	ND	5 ± 2	ND

[a] Processive incorporation of multiple dNTPs into a duplex DNA substrate was performed as described in Materials and Methods. Rate constants for DNA polymerization and nonproductive complex formation were determined using KINSIM computer simulation (*18*) of the data to the model presented in Scheme 1. [b] Rate constant for primer extension. [c] Rate constant for intermediate product formation. [d] Not determined as extension beyond these positions was not detected as a result of nucleotide triphosphate omission.

Table 4: Summary of Equilibrium Binding Constants of EIAV RT for 25/36-mer, 30/60-mer, and 36/60-mer DNA Substrates[a]

	25/36-mer	30/60-mer	36/60-mer
K_d (nM)	12 ± 2	23 ± 4	36 ± 6
amplitude[b] (nM)	20	20	15
% enzyme[c]	100	100	75

[a] Titrations were performed using a filter binding assay as described in Materials and Methods. [b] Amplitude refers to the maximal value of the enzyme−nucleic acid complex and is not an indication of the functional enzyme−DNA complex. [c] Percent enzyme was obtained by dividing the amplitude of the enzyme−DNA complex by the concentration of enzyme used per experiment.

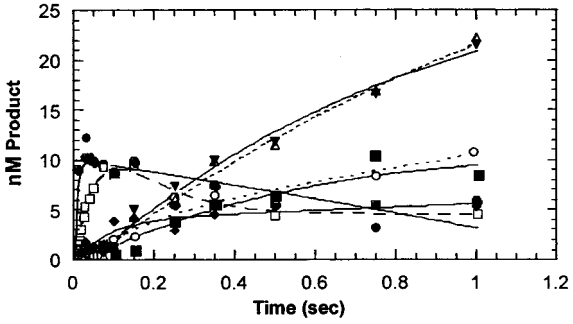

FIGURE 5: Processive DNA synthesis by EIAV RT using the 30/60-mer DNA substrate. Product formation is denoted as follows: ● = +1 product, □ = +2 product, ◆ = +3 product, ○ = +4 product, ▼ = +5 product, △ = +6 product, and ■ = +7 product. The curves for product formation were generated using the rate constants denoted in Table 3, which were obtained through computer simulation of the experimental data to Scheme 1.

for the dissociation of EIAV RT during polymerization through the CTS using a trap extension assay. EIAV RT (300 nM) and ^{32}P-labeled 30/60-mer substrate (300 nM) were preincubated and mixed with a saturating amount of dCTP and dATP (100 μM each) and a large excess of ^{32}P-end-labeled 25/36-mer DNA (3 μM) serving as the "extendable" trap.

The observed lag of approximately 500 ms before trap extension (Figure 6A) has two important mechanistic ramifications. First, the lag indicates that all RT is initially bound to the 30/60-mer DNA substrate, although the low amplitudes in product formation indicate that the majority of enzyme is bound nonproductively. Thus, the rate of trap extension must

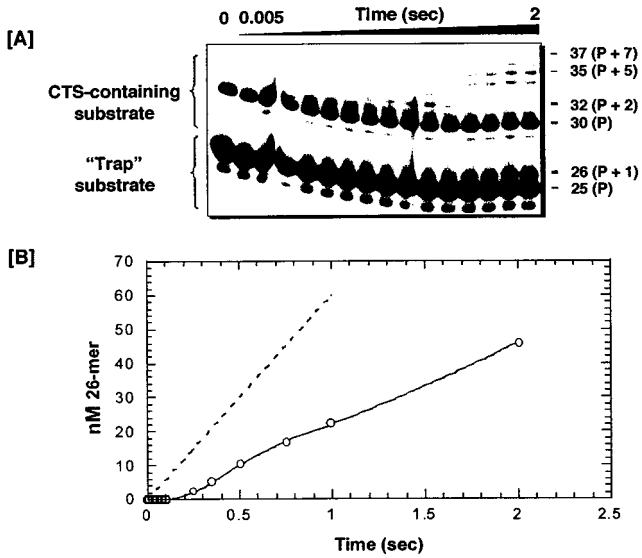

FIGURE 6: Detection of RT dissociation during processive replication through the CTS. (A) Reaction products separated on a 16% denaturing polyacrylamide gel. 300 nM RT preincubated with 300 nM 30/60-mer (CTS-containing substrate) was rapidly mixed with 3 μM trap substrate and dCTP and dATP (100 μM final concentration) for times ranging from 5 to 2000 ms. The trap substrate was 25/36-mer whose 25-mer primer was 5′-labeled. For convenience, only the initial substrate (P) and extended product (P + 2, P + 5, and P + 7, respectively) are denoted for extension of the CTS-containing substrate. Reaction products for trap substrate extension are denoted as P and P + 1, respectively. (B) Time course for extension of the 25/36-mer DNA trap. The solid line demonstrates the lag in product formation while the dashed line represents the theoretical curve in trap extension if k_{int} reflects the rate of enzyme dissociation.

be limited by dissociation of RT from either the 30/60-mer substrate or any intermediate products formed. Second, the lag in trap extension correlates well with the time frame in which all DNA synthesis is halted during replication through the CTS (Figure 6). As will be more thoroughly discussed later, the lag in trap extension indicates that the k_{off} of RT from the nonextendable products must be slower than the "fast" rates defining intermediate product formation. The presence of trap does not affect extension of 30/60-mer since the rates of elongation and intermediate product formation are identical to those measured in the absence of DNA trap. Similar results, i.e., a lag of approximately 500 ms before observation of trap extension, were obtained when RT was challenged with strand displacement DNA synthesis (data not shown).

Equilibrium Binding Constants of EIAV RT for Various DNA Substrates. A filter binding assay was used to define the equilibrium binding constant (K_d) of RT for 25/36-mer, 30/60-mer, and 36/60-mer substrates. The 36/60-mer substrate is analogous to the +6 product of a 30/60-mer processive extension reaction and, therefore, has the same sequence as a Ter 1 termination product that accumulates in the pre-steady-state experiments. Binding isotherms for all DNA substrates are presented in Figure 7. The K_d value of 12 ± 1 nM for the 25/36-mer is in excellent agreement with 4.7 and 10 nM reported for HIV-1 RT using DNA of random sequence (*21*, *22*). K_d values of 22 ± 3 and 36 ± 6 nM were obtained for the 30/60-mer CTS and 36/60-mer termination substrates, respectively. Thus, the apparent binding affinity of RT for CTS-containing substrates is

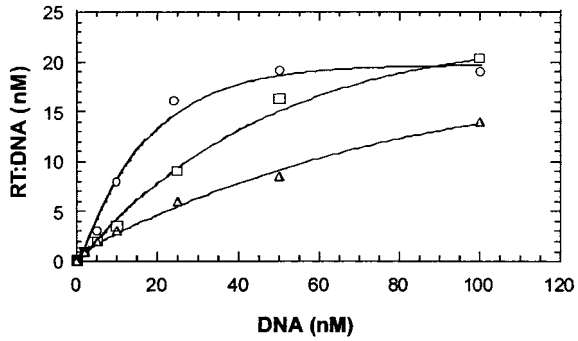

FIGURE 7: Binding isotherms of EIAV RT for 25/36-mer (○), 30/60-mer (□), and 36/60-mer (△) DNA substrates.

approximately 2−3-fold lower than for DNA of random sequence. The binding isotherms also reveal a maximal RT−DNA concentration of 20 nM, equal to the final concentration of RT, using 25/36-mer and 30/60-mer. By contrast, a maximal RT−DNA concentration of ~15 nM is obtained using 36/60-mer, indicating that approximately 75% of RT can bind to this DNA substrate.

DISCUSSION

Retroviral DNA replication is mediated by a variety of *cis*-acting sequences and *trans*-acting factors (*27*). The most extensively studied *cis*-acting sequences include the distinct conformations of RNA/RNA, DNA/RNA, and DNA/DNA substrates encountered during replication. However, another element, defined as the CTS, plays an important role in terminating lentiviral DNA replication (*11*). We have evaluated the molecular events inducing sequence-specific termination through pre-steady-state techniques to measure the rate constants defining several of the microscopic kinetic events catalyzed by RT during DNA polymerization. Our analysis is divided into two sections to highlight the mechanistic ramifications of this unique element.

Mechanism of Single Nucleotide Incorporation. The kinetics of single nucleotide polymerization using the variety of DNA substrates displayed in Figure 1 were all biphasic, indicating that a step after chemistry, most likely release of enzyme from extended DNA, is the rate-limiting step for enzyme turnover (*17*). While rate constants for initial product formation (k_{obs}) are independent of DNA sequence (~30 s^{-1}), the burst amplitude, reflecting the amount of functional RT−DNA complex, was. For example, the burst amplitude with 30/60/44-mer is 50% lower than in the absence of the displacement strand. More surprising is the fact that the burst amplitude using 30/60-mer is 50% lower than that using the 25/36-mer control substrate. The reduction in burst amplitudes suggests that RT cannot bind as tightly to CTS-containing DNA as compared to DNA of random sequence. However, the nearly identical k_{obs} values obtained using the three DNA substrates indicate that whatever fraction of RT is bound to DNA is catalytically active regardless of DNA sequence.

At face value, the lower burst amplitudes are consistent with a weaker binding affinity of RT for CTS-containing substrates. Indeed, the K_d for 30/60-mer substrate is 2-fold higher compared to the 25/36-mer control substrate (25 versus 12 nM). However, this cannot account entirely for the 50% reduction in burst amplitude. Using the aforementioned K_d values and reaction conditions employed for active site titrations, ~98% of RT should be bound to the 25/36-mer while ~91% of RT should be bound to the 30/60-mer. Thus, nearly identical burst amplitudes would be expected regardless of DNA substrate. This discrepancy suggests that perturbations in ground state binding of DNA to RT are not solely responsible for the reduced burst amplitudes. Instead, nearly 100% of enzyme is capable of binding the DNA substrates while only a fraction is catalytically "competent" to rapidly incorporate a dNTP to yield a burst in product formation. Consistent with this interpretation, filter binding assays also demonstrate that 100% of RT is capable of binding to either 25/36-mer or 30/60-mer.

Steady-state rates of nucleotide incorporation vary as a function of DNA substrate. The biphasic nature of the time course in single nucleotide incorporation indicates that a step after phosphoryl transfer is rate-limiting for enzyme turnover. This rate-limiting step has been ascribed as release of enzyme from product DNA (k_{off}) and is equivalent to k_{cat} (*17*). The subsequent increase in k_{cat} values indicates that enzyme dissociation is faster with CTS-containing substrates compared to DNA of random sequence (Table 1). Closer inspection reveals that k_{cat} using the 30/60-mer is 2-fold faster than that using the 25/36-mer substrate. This parallels the 2-fold higher K_d for the 30/60-mer. Assuming that k_{on} is unaffected by DNA sequence and is ~2×10^7 M^{-1} s^{-1} (*23*), k_{off} values of RT from 25/36-mer and 30/60-mer are estimated to be 0.24 and 0.48 s^{-1}, respectively, and in excellent agreement with the k_{cat} values of 0.28 and 0.60 s^{-1} for 25/36-mer and 30/60-mer, respectively, measured through the time courses in single nucleotide incorporation.[3]

It is tempting to speculate that the poly A-tract of the CTS causes the reduction in burst amplitudes. This appears unlikely since active site titrations of EIAV RT using the 30/41-mer hybrid DNA also yield a 50% decrease in the expected burst amplitude. Since this duplex does not contain the poly A-tract of the CTS, the diminished burst amplitudes most likely result from interactions between EIAV RT and the region of DNA upstream of the CTS and not its T_6-tract. As before, the k_{obs} of 33 ± 3 s^{-1} indicates that the functional RT−DNA complex is unperturbed with regard to dNTP incorporation. However, the k_{cat} value using the 30/41-mer is identical to that obtained using the 25/36-mer, indicating that k_{off} is not affected by this substrate. As an additional control, the time course in dCTP incorporation by EIAV RT was measured using the 34/62-mer DNA substrate which is devoid of both the CTS and upstream DNA sequence. The amplitude in initial product formation and the rate constants for initial product formation and enzyme turnover are nearly identical to those using the 25/36-mer DNA substrate. These data argue that the observed differences in kinetic behavior by EIAV RT are not caused by potential effects mediated by primer/template length. Instead, the kinetic and filter binding data collectively indicate that specific contacts between RT and the duplex DNA region immediately upstream of the CTS contribute to nonproductive complex formation to lower the functional concentration

[3] This analysis assumes that the steady-state rate in dCTP incorporation is limited by the release of enzyme from extended DNA and not by a kinetic step after phosphoryl transfer such as a conformational change, pyrophosphate release, or enzyme translocation.

of RT−DNA. It is possible that the sequence immediately upstream of the CTS may have evolved to enhance termination. Consistent with this hypothesis, the HIV-1 CTS has a weak termination sequence (Ter 1) immediately upstream of the strong HIV-1 termination sequence (Ter 2) that may serve a similar function.

The effects of the DNA sequence encompassing the CTS are not limited to EIAV RT since active site titrations of Klenow fragment and HIV-1 RT yield similar results. It is not surprising that HIV-1 RT is sensitive since it is functionally identical and analogous termination sequences are present in the HIV genome (*8*). It is, however, somewhat surprising that Klenow fragment shows similar sensitivity and suggests that other DNA polymerases are also sensitive to the same contextual and, presumably, structural perturbations of the CTS. Evaluating the efficiency of eukaryotic DNA replication using CTS-containing DNA will be an important area of inquiry since eukaryotic DNA and RNA polymerases must polymerize through the CTS during replication and viral mRNA synthesis following infection and integration of proviral DNA.

Molecular Consequences of Processive DNA Replication through the CTS. Quantitative evaluation of processive DNA synthesis on the 25/36-mer control substrate and the CTS-containing 30/60-mer indicates that this occurs in a sequential and time-dependent manner as initial substrate is converted to product. Similar to that observed for HIV-1 RT (*21*), the time course in processive DNA replication catalyzed by EIAV RT reveals intermediate products which are not completely converted to full-length product. This is exemplified by the successive lowering of the amplitudes in product formation corresponding to positions +2, +3, +4, etc. Using global fit analysis, the rates of extension and intermediate product formation were defined by fitting the time courses in product formation to Scheme 1. Rate constants for extension are approximately 25 s^{-1} using either the 25/36-mer or the CTS-containing 30/60-mer. The identity in rate constants indicates that the A-tract region of the CTS does not significantly perturb the efficiency of nucleotide incorporation. However, intermediate products are not completely converted to full-length product, and this may be caused by rapid dissociation of enzyme from the extending DNA or the formation of nonproductive RT−DNA complexes. As indicated in Table 2, values of k_{int} progressively increase as RT replicates through a CTS-containing (30/60-mer) and control DNA substrate (25/36-mer). However, pausing at the +5 and +6 products using the CTS-containing substrate results from a dramatic increase in k_{int} compared to the rate of polymerization at the same positions. In fact, the rate constant of intermediate product formation at +5 is only 2-fold lower than the rate constant of polymerization to yield +6 product (k_{int} = 17 s^{-1} versus k_{ext} = 30 s^{-1}). In contrast, the rate at +6 is 1.5-fold higher than the rate of polymerization to yield +7 product (k_{int} = 45 s^{-1} versus k_{ext} = 30 s^{-1}). At the molecular level, the high k_{int}/k_{ext} ratio reflects RT partitioning into a nonfunctional complex at a higher frequency to cause pausing. It is important to note that while the rate constants of intermediate product formation do successively increase using the 25/36-mer substrate, the ratio of k_{int}/k_{ext} is always less than 0.3. Thus, the frequency at which RT pauses at random DNA sequences is low. Support for this mechanism is provided by the enzyme's ability to fully extend the 25/36-mer when supplied with all four dNTPs while extension of the 30/60-mer substrate still accumulated +5 and +6 products.

It is important to note that these nonproductive complexes are, in one context, reversible since RT is capable of dissociating from the sequences and reinitiating DNA synthesis. However, the data presented indicate that the enzyme dissociates and then can rebind so that DNA synthesis can occur from these DNA sequences within the A_6-tract of the CTS. This is consistent with the previously reported steady-state characterization which demonstrated that although EIAV RT paused at the CTS, the enzyme was capable of extending beyond this sequence (*11*). However, the time frame for extension beyond the CTS is on the order of minutes whereas this study shows definitive pausing on the millisecond to second time scale.

In vivo, RT must displace DNA through the CTS during late (+) strand DNA synthesis. The displacement strand may actively participate during termination by providing a physical barrier to perturb RT binding and/or translocation. Alternatively, the displacement strand may play a passive role by simply preventing the rebinding of enzyme. The kinetic data presented in Table 2 indicate that the rates of DNA polymerization using the 30/60/44-mer substrate are approximately 2-fold lower than those obtained using the 30/60-mer substrate. Similar to replication in the absence of strand displacement, rate constants for intermediate product formation again increase as RT polymerizes through the CTS. However, the identity in rate constants indicates that strand displacement does not enhance the rate of intermediate product formation. Termination occurs at the +4 and +5 products due to an increase in the k_{int}/k_{ext} ratio which results primarily through a decrease in the rate of extension, indicating that the displacement strand first plays an active role in terminating synthesis at the CTS by decreasing the rate of polymerization. Although not directly tested, the displacement strand presumably plays a passive role by eclipsing the 3′-hydroxyl of the primer to prevent the renewal of DNA synthesis at the CTS. This may possibly explain the 50% reduction in burst amplitude observed in the active site titrations.

By measuring processive synthesis through CTS-containing DNA substrates concomitantly with extension of a DNA trap, we demonstrated that the structural features enhance formation of nonproductive RT−DNA complexes without enhancing dissociation. Although RT does dissociate from the CTS, extension of the DNA trap does not occur until replication through the CTS-containing substrate has halted at the predominant termination sites. If RT had rapidly dissociated from the intermediary replication products as governed by the rate constants summarized in Table 3, extension of the DNA trap should likewise had been rapid. However, the lag in trap extension correlates with the time frame of "pausing" on the CTS-containing DNA substrate, indicating that RT remains bound in a nonproductive complex. Furthermore, extension of the trap demonstrates that the enzyme does not remain bound indefinitely to the intermediate products, ruling out its participation in translocation of the genome across the nuclear membrane or in recruiting factors for nuclear transport.

Conclusions. From our data, we propose a mechanism underlying the molecular basis of pausing and termination

Scheme 2: Model for Discontinuous Plus Strand Synthesis[a]

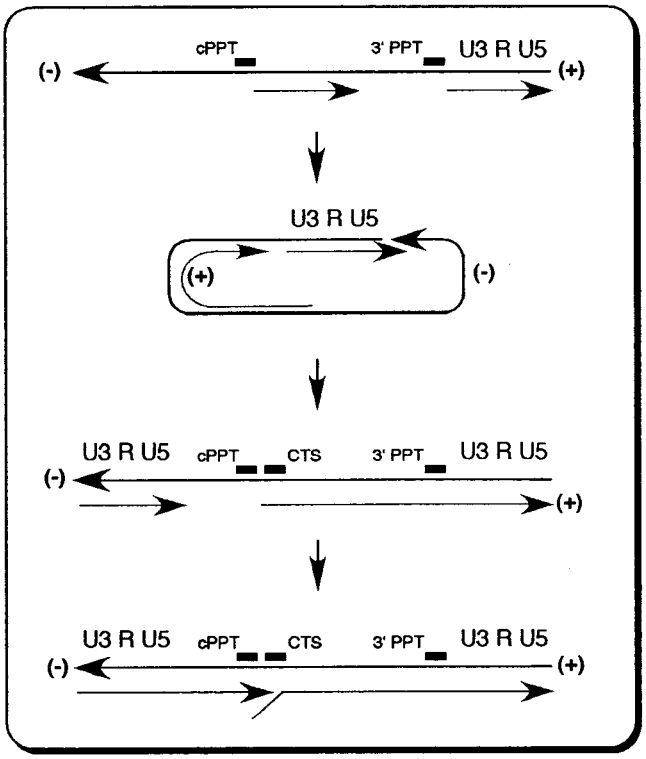

[a] EIAV (+) strand DNA synthesis proceeds from two independent priming events occurring at the cPPT and the 3′-PPT. Following strand transfer, the plus strand segment primed from the 3′-PPT is extended by RT until it reaches the 3′ terminus of the segment primed from the cPPT. A mechanism to terminate DNA synthesis of RT on this upstream segment is thus required to prevent displacement of the cPPT primed downstream segment of plus strand DNA. The location of the EIAV CTS is indicated by an asterisk (*).

of lentiviral DNA replication induced by the CTS, a unique in vivo relevant DNA sequence. In Scheme 2, RT is bound to the primer terminus located directly upstream from the CTS. Although nearly 100% of the enzyme can bind to this substrate with high affinity, the reduced burst in initial product formation indicates that a fraction is either inactive or nonproductively bound. As replication proceeds through the A-tract of CTS, the enzyme progressively becomes "forced" into nonproductive complexes at an enhanced rate. This is likely caused by changes in the conformational structure of the newly replicated A-tract region of the CTS since the newly formed A/T duplex is prone to curvature induced by minor groove compression (*11*). DNA synthesis is terminated when the enzyme replicates up to positions A4 and A5 of the CTS. The ramifications of this mechanism are truly fascinating since the enzyme creates an altered DNA structure, forcing the enzyme into a nonproductive complex. As RT encounters the displacement strand during late (+) strand DNA synthesis, the rate of polymerization is slowed 2-fold although the rate of nonproductive complex formation is not significantly enhanced. As was the case during early (+) strand DNA synthesis, the increased partitioning of the enzyme into nonproductive complexes causes termination. However, complete termination during late (+) strand DNA synthesis is likely caused by the displacement strand eclipsing the 3′-hydroxyl of the primer.

A large collection of pre-steady-state kinetic investigations with HIV-1 reverse transcriptase (HIV-1 RT) have reported bursts of 30−50% of product formation in the initial reaction cycle using unaltered nucleic acid substrates (*21*−*23*). However, the presence of carcinogen adducts and other modified DNA lesions as well as secondary structure in the template has also been demonstrated to alter polymerase fidelity and/or activity (*28*−*32*). For example, Furge and Guengerich have observed substoichiometric burst amplitudes during nucleotide addition by HIV-1 RT in the presence of 8-oxoGua in template DNA (*28*, *29*). By using computer simulation, these authors were able to expand the minimal kinetic mechanism of HIV-1 RT to include the formation of nonproductive enzyme−nucleic acid complexes to account for substoichiometric burst amplitudes in initial product formation (*29*). Likewise, Suo et al. (*30*) have also demonstrated that nucleotide addition by HIV-1 RT in the presence of a single *cis*-platin DNA intrastrand cross-link proceeds via productive and nonproductive enzyme−DNA complexes, of which the latter can isomerize into a productive form. More relevant to the results of this paper is the quantitative examination of alternative enzyme kinetics and mechanism for HIV-1 RT using RNA and DNA substrates with secondary structure (*31*, *32*). This study demonstrated reductions in burst amplitude without reduced burst rate, thereby indicating that pausing of retroviral DNA can proceed through nonproductive nucleic acid substrate binding and not enzyme dissociation. The results presented in this paper are consistent with these previously published reports and expand our understanding of the dynamics of retroviral replication, specifically with regard to the in vivo ramifications of repetitive DNA sequences such as the CTS.

The dramatic effects of A-tract DNA toward modulating the efficiency of lentiviral replication are surprising since RT must efficiently utilize a variety of nucleic acid substrates. Structural data reveal a deep cleft in the polymerase domain of p66 which comprises the nucleic acid binding site (*33*, *34*). Specific regions of the enzyme, including the "template grip" (*35*) and the "primer grip" (*36*), have been implicated as sites of significant interactions with the primer/template. Of particular significance is how these regions "contort" the nucleic acid substrate for proper utilization. The structure of HIV-1 RT complexed with duplex DNA reveals that DNA in the vicinity of the polymerase active site is in an A-form helix as opposed to the expected B-form (*37*). The choice of the A-form DNA may be dictated by the fact that although the DNA/DNA duplex can assume an A-form structure, an RNA/RNA duplex cannot assume a B-form structure. Thus, all nucleic acid substrates may be constrained to assume the A-form so that the enzyme may accommodate RNA/RNA, DNA/RNA, and DNA/DNA. It is tempting to speculate that the A/T duplex of the CTS cannot adopt the required A-form conformation. As a result, the enzyme can still bind the nucleic acid substrate but is unable to switch the conformation of the DNA to a usable form, thus leading to the formation of nonproductive RT−DNA complexes.

ACKNOWLEDGMENT

We deeply appreciate the generosity of Dr. Birgit Wohrl for supplying the EIAV RT used in this study.

SUPPORTING INFORMATION AVAILABLE

Kinetic analyses using KINSIM for time courses in single nucleotide addition, in processive DNA replication, and in

monitoring enzyme dissociation during processive DNA replication. This material is available free of charge via the Internet at http://pubs.acs.org.

REFERENCES

1. Finston, W. I., and Champoux, J. J. (1984) *J. Virol. 51*, 26−33.
2. Pullen, K. A., and Champoux, J. J. (1990) *J. Virol. 64*, 6274−6274.
3. Sorge, J., and Hughes, S. H. (1982) *J. Virol. 43*, 482−488.
4. Hungnes, O., Tjotta, E., and Grinde, B. (1992) *Virology 190*, 440−442.
5. Charneau, P., Mirambeau, G., Roux, P., Paulous, S., Buc, H., and Clavel, F. (1994) *J. Mol. Biol. 241*, 651−662.
6. Arts, E. J., and Le Grice, S. F. (1998) *Prog. Nucleic Acid Res. Mol. Biol. 58*, 339−393.
7. Rumbaugh, J. A., Fuentes, G. M., and Bambara, R. A. (1998) *J. Biol. Chem. 273*, 28740−28745.
8. Charneau, P., and Clavel, F. (1991) *J. Virol. 65*, 2415−2421.
9. Lavigne, M., Roux, P., Buc, H., and Schaeffer, F. (1997) *J. Mol. Biol. 266*, 507−524.
10. Lavigne, M., and Buc, H. (1999) *J. Mol. Biol. 285*, 977−995.
11. Stetor, S. R., Rausch, J. W., Guo, M.-J., Burnham, J. P., Boone, L. R., Waring, M. J., and LeGrice, S. F. L. (1999) *Biochemistry 38*, 3656−3667.
12. Souquet, M., Restle, T., Krebs, R., LeGrice, S. F. J., Goody, R., and Worhl, B. (1998) *Biochemistry 37*, 12144−12152.
13. Wohrl, B. M., Howard, K. J., Jacques, P. S., and Le Grice, S. F. (1994) *J. Biol. Chem. 269*, 8541−8548.
14. Joyce, C. M., and Derbyshire, V. (1995) *Methods Enzymol. 262*, 3−13.
15. Kuchta, R. D., Mizrahi, V., Benkovic, P. A., Johnson, K. A., and Benkovic, S. J. (1987) *Biochemistry 26*, 8410−8417.
16. Wong, I., Patel, S. S., and Johnson, K. A. (1991) *Biochemistry 30*, 526−537.
17. Johnson, K. A. (1986) *Methods Enzymol. 134*, 677−705.
18. Barshop, B. A., Wrenn, R. F., and Frieden, C. (1983) *Anal. Biochem. 130*, 134−145.
19. Wong, I., and Lohman, T. M. (1993) *Proc. Natl. Acad. Sci. U.S.A. 90*, 5428−5432.
20. Suo, Z., and Johnson, K. A. (1997) *Biochemistry 36*, 12459−12467.
21. Kati, W. M., Johnson, K. A., Jerva, L. F., and Anderson, K. S. (1992) *J. Biol. Chem. 267*, 25988−25997.
22. Beard, W. A., Bebenek, K., Darden, T. A., Li, L., Prasad, R., Kunkel, T. A., and Wilson, S. H. (1998) *J. Biol. Chem. 273*, 30435−30442.
23. Reardon, J. E. (1993) *J. Biol. Chem. 268*, 8743−8751.
24. di Marzo Veronese, F., Copeland, T. D., DeVico, A. L., Rahman, R., Oroszlan, S., Gallo, R. C., and Sarngadharan, M. G. (1986) *Science 231*, 1289−1291.
25. Lightfoote, M. M., Coligan, J. E., Folks, T. M., Fauci, A. S., Martin, M. A., and Venkatesan, S. (1986) *J. Virol. 60*, 771−775.
26. Tozser, J., Friedman, D., Weber, I. T., Blaha, I., and Oroszlan, S. (1993) *Biochemistry 32*, 3347−3353.
27. Rosen, C. A. (1991) *Trends Genet. 7*, 9−14.
28. Furge, L. L., and Guengerich, F. P. (1997) *Biochemistry 36*, 6475−6487.
29. Furge, L. L., and Guengerich, F. P. (1999) *Biochemistry 38*, 4818−4825.
30. Suo, Z., Lippard, S. L., and Johnson, K. A. (1999) *Biochemistry 38*, 715−726.
31. Suo, Z., and Johnson, K. A. (1997) *Biochemistry 36*, 12459−12467.
32. Suo, Z., and Johnson, K. A. (1998) *J. Biol. Chem. 273*, 27259−27267.
33. Kohlstaedt, L. A., Wang, J., Friedman, J. M., Rice, P. A., and Steitz, T. A. (1992) *Science 256*, 1783−1790.
34. Jacobo-Molina, A., Ding, J., Nanni, R. G., Clark, A. D., Jr., Lu, X., Tantillo, C., Williams, R. L., Kamer, G., Ferris, A. L., and Clark, P. (1993) *Proc. Natl. Acad. Sci. U.S.A. 90*, 6320−6324.
35. Ghosh, M., Williams, J., Powell, M. D., Levin, J. G., and LeGrice, S. F. L. (1997) *Biochemistry 36*, 5758−5768.
36. Wohrl, B. M., Krebs, R., Thrall, S. H., LeGrice, S. F. L., Scheidig, A. J., and Goody, R. S. (1997) *J. Biol. Chem. 272*, 17581−17587.
37. Huang, H., Chopra, R., Verdine, G. L., and Harrison, S. C. (1998) *Science 282*, 1669−1675.

BI010354I